

## Supporting Information

### **A near-infrared fluorescent probe that can image endogenous hydrogen polysulfides in vivo in tumour-bearing mice**

Ling Zhang, <sup>\*a, b</sup> Huizhen Liu,<sup>a</sup> Chunli Wu,<sup>a</sup> Youguang Zheng,<sup>a</sup> Xiaoning Kai,<sup>a</sup> and Yunsheng Xue<sup>a\*</sup>

<sup>a</sup>Jiangsu Key Laboratory of New Drug Research and Clinical Pharmacy, Jiangsu Center for the Collaboration and Innovation of Cancer Biotherapy, School of Pharmacy, Xuzhou Medical University, Xuzhou 221002, PR China.

<sup>b</sup>NHC Key Laboratory of Nuclear Medicine, Jiangsu Key Laboratory of Molecular Nuclear Medicine, Jiangsu Institute of Nuclear Medicine, Wuxi 214063, PR China.

## **General Information**

### **Synthesis and Characterisation of compounds**

### **Absorption analyses**

### **Evidence of mechanism detection**

### **Determination of the detection limit**

### **Quantum Yields**

### **MTT assay**

### **Preparation of the test solution**

### **References**

**Scheme S1. Response mechanism of NIR-CPS to  $H_2S_n$ .**

**Scheme S2. Synthetic route of NIR-CPS.**

**Figure S1. Absorption spectra and fluorescence spectra of NIR-CPS.**

**Figure S2. Fluorescence spectra of NIR-COH and NIR-CPS in PBS buffer, DMSO, Acetonitrile.**

**Figure S3. Absorption spectra of NIR-COH and NIR-CPS in PBS buffer, DMSO, Acetonitrile.**

**Figure S4. Time profile of NIR-CPS towards  $H_2S_n$ .**

**Figure S5. Effects of pH on NIR-CPS in PBS buffer.**

**Figure S6. Fluorescence intensities of NIR-CPS in PBS buffer for 10, 20, 30, 40, 50 and 60 min.**

**Figure S7. Selectivity of NIR-CPS to reactive oxygen species and reactive nitrogen species.**

**Figure S8. Selectivity of NIR-CPS to various ions.**

**Figure S9. Cell viability of different concentrations of NIR-CPS in MCF-7 cells.**

**Figure S10. Cell viability of NIR-CPS at different times in MCF-7 cells.**

**Figure S11. The corresponding bright images of Fig. 3.**

**Figure S12. The corresponding bright images of Fig. 4.**

**Figure S13. Fluorescence images of visualizing  $H_2S_n$  levels at different times in living mice using NIR-CPS.**

**Figure S14.  $^1H$  NMR spectrum of compound 2.**

**Figure S15.  $^{13}C$  NMR spectrum of compound 2.**

**Figure S16.  $^1H$  NMR spectrum of NIR-CPS.**

**Figure S17.  $^{13}C$  NMR spectrum of compound NIR-CPS.**

**Figure S18. HR-MS identification of NIR-CPS.**

**Figure S19.  $^1H$  NMR spectrum of NIR-COH.**

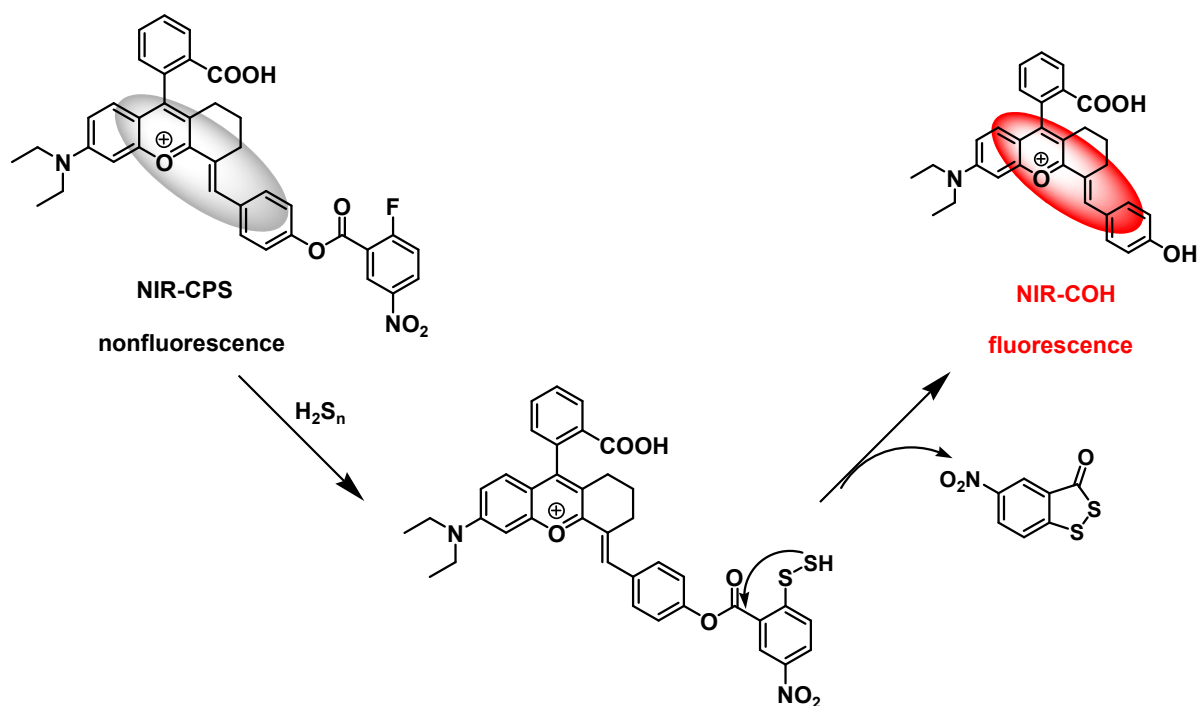
**Figure S20. HR-MS identification of NIR-COH.**

**Figure S21.  $^1H$  NMR spectra of the isolated fluorescent product of NIR-CPS +  $Na_2S_4$ .**

**Figure S22. HR-MS identification of isolated fluorescent product of NIR-CPS +  $Na_2S_4$ .**

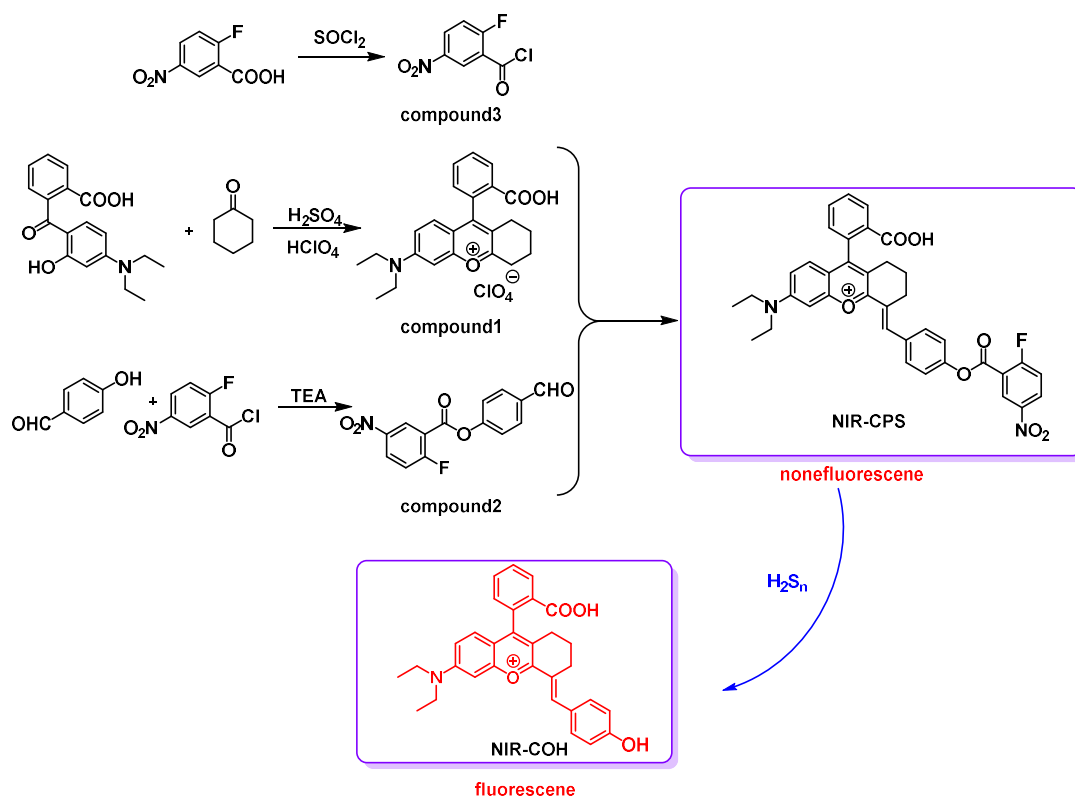
**Table S1. Summary of the reported  $H_2S_n$  fluorescent probes.**

**General Information.** Thin layer chromatography was performed on silica gel 60 F<sub>254</sub> plates (250 μm) and column chromatography was conducted over silica gel (300-400 mesh). Visualization of the developed chromatogram was accomplished by a UV lamp. Unless noted otherwise, reagents and solvents were obtained from commercial suppliers and employed without further purification. Nuclear magnetic resonance (NMR) spectra were obtained on JEOL ECZ-400S operated at 400/100 MHz for <sup>1</sup>H NMR and <sup>13</sup>C NMR, respectively. High-resolution mass spectra (HRMS) were measured by using a mass spectrometer. The pH measurements were measured with a Mettler-Toledo Delta 320 pH meter. Absorbance in the MTT assay was recorded using a spectrophotometer (Thermo Fisher Scientific, Finland). All fluorescence measurements were recorded on a Hitachi F4600 Fluorescence Spectrophotometer. All fluorescence imaging experiments were conducted on a FV1000 confocal laser scanning microscope (Olympus, Japan). The in vivo imaging was performed using a Night OWL IILB 983 small animal in vivo imaging system.



**Scheme S1.** Response mechanism of NIR-CPS to H<sub>2</sub>S<sub>n</sub>.

## Synthesis and Characterisation of compounds.



Scheme S2. Synthetic route of NIR-CPS.

**Synthesis of compound 2.** Compound 2 was synthesized according to the method reported by Liu et al.<sup>1</sup> *p*-hydroxybenzaldehyde (0.2 g, 1.64 mmol) was dissolved in 20 mL dichloromethane followed by the addition of triethylamine (274.1  $\mu\text{L}$ , 1.97 mmol) to the solution. The mixture was cooled in an ice-bath and then 2-fluoro 5-nitrobenzoyl chloride (0.4 g, 1.97 mmol) in 10 mL dichloromethane was added dropwise. The mixture was stirred at 0 °C for 30 min, and then stirred at room temperature for 1 h. The solvent was removed under reduced pressure to obtain the crude product. The crude product was purified by recrystallization with ethyl acetate (20 mL) to afford compound 2 (0.36 g, 75.1 %). TLC (silica, PE:EA, 5:1 v/v):  $R_f = 0.5$ .  $^1\text{H NMR}$  (400 MHz,  $\text{CDCl}_3$ ):  $\delta$  10.04 (s, 1H), 9.01 (dd,  $J = 6.0$ ,  $J = 2.8$  Hz, 1H), 8.49–8.53 (m, 1H), 7.98–8.01 (m, 2H), 7.40–7.46 (m, 3H).  $^{13}\text{C NMR}$  (100 MHz,  $\text{CDCl}_3$ ):  $\delta$  190.82, 166.90, 164.12, 160.05, 154.71, 134.68, 131.47, 130.72, 130.59, 128.70, 128.68, 122.37, 119.06, 118.96.

**Synthesis of NIR-COH.** Compound 1 (0.2 g, 0.53 mmol), 4-hydroxybenzaldehyde (77.90 mg, 0.64 mmol) and piperidine (5.2  $\mu\text{L}$ , 0.05 mmol) dissolved in dry ethanol (15 mL). The mixture was reflux for 5 h. The solvent was removed under reduced pressure, then the crude product was dissolved in 60 mL dichloromethane, washed with 30 mL water. The crude product was purified by silica gel column to afford

compound NIR-COH as a black solid (145 mg, 56.8 %). TLC (silica, CH<sub>2</sub>Cl<sub>2</sub>:CH<sub>3</sub>OH, 10:1 v/v) :R<sub>f</sub>= 0.4. <sup>1</sup>H NMR (400 MHz, CD<sub>3</sub>OD): δ 8.18-8.20 (m, 1H), 8.11 (s, 1H), 7.64-7.73 (m, 2H), 7.56 (d, *J* = 8.8 Hz, 2H), 7.21-7.24 (m, 1H), 7.18 (t, *J* = 2.0 Hz, 1H), 7.09-7.15(m, 2H) 6.89 (d, *J* = 8.8 Hz, 2H), 3.67 (q, *J* = 7.2 Hz, *J* = 14.4 Hz, 4H), 2.93-2.97 (m, 2H), 2.40-2.44 (m, 2H), 1.78-1.85 (m, 2H), 1.29 (t, *J* = 7.2 Hz, 6H). HRMS(ESI<sup>+</sup>): (M<sup>+</sup>)calcd. for C<sub>31</sub>H<sub>30</sub>NO<sub>4</sub>, 480.2169; found, 480.2170.

**Absorption analyses.** UV-Vis absorption spectra were detected at room temperature on a Shimadzu PharmaSpec UV-2401PC UV-Visible spectrophotometer. NIR-CPS probe solution (DMSO) was added to a quartz cuvette. With the probe diluted to 10 μM with 20 mM PBS buffer, Na<sub>2</sub>S<sub>4</sub> was added. The resulting solution was incubated for 20 min prior to measurements (n = 3), with the mean ± SD expressed.

**Evidence of mechanism detection.** NIR-CPS (64.70 mg, 0.10 mmol) was dissolved in DMSO (15 mL), and then the solution of Na<sub>2</sub>S<sub>4</sub> (348 mg, 2.0 mmol) in PBS buffer (30 mL, 20 mM, pH = 7.4) was added. After stirring at 37 °C for 30 min, the resultant mixture was extracted by EtOAc. The fluorescent product was thereafter purified by column chromatography and further characterised by HRMS and <sup>1</sup>H NMR. The NMR and HRMS spectra of fluorescent product were consistent with those of compound NIR-COH, hence confirmation of the fluorescent product as compound NIR-COH.

**Determination of the detection limit.** The detection limit was calculated based on previous method.<sup>2</sup> The fluorescence emission spectrum of NIR-CPS without Na<sub>2</sub>S<sub>4</sub> was measured by 10 times and the standard deviation of blank measurement was determined. Then the probe solution was added with Na<sub>2</sub>S<sub>4</sub> of concentration from 0 to 20 μM. A linear regression curve was then achieved according to the fluorescence intensity in the range of Na<sub>2</sub>S<sub>4</sub> from 0 to 20 μM. The detection limit was calculated with the following equation: Detection limit = 3σ/k. Where σ is the standard deviation of blank measurements, k is the slope between the fluorescence intensity ratios versus Na<sub>2</sub>S<sub>4</sub> concentrations.

**Quantum Yields.** Quantum yields were determined by using ICG as fluorescence standard (Φ<sub>f</sub> = 0.13 in DMSO). The quantum yield was calculated according to the equation: Φ<sub>sample</sub> = Φ<sub>standard</sub> (Grad<sub>sample</sub>/Grad<sub>standard</sub>)(η<sup>2</sup><sub>sample</sub>/η<sup>2</sup><sub>standard</sub>); where Φ is the quantum yield, Grad is the slope of the plot of absorbance versus integrated emission intensity, and η is the refractive index of the solvent. Absorbance of sample and standard at their respective excitation wavelengths was kept below 0.05.

**MTT assay.** The in vitro cytotoxicity of NIR-CPS were measured using a colorimetric MTT assay kit (Sigma-Aldrich). MCF-7 cells were seeded in 96-well plates at a density of 50,000 cells/well and then maintained at 37 °C in a 5 % CO<sub>2</sub> incubator. The cells were incubated with different concentrations of NIR-CPS for 24 h, respectively. Cells in culture medium without NIR-CPS were used as control. After the incubation time, 20 μL of MTT dye (3-[4, 5-dimethylthiazol-2-yl]- 2, 5-diphenyl tetrazolium bromide, 5 mg/ml in phosphate buffered saline), was added to each well, and the plates were incubated for 4 h at 37

°C. Then, the remaining MTT solution was removed, and 150  $\mu$ L of DMSO was added to each well to dissolve the formazan crystals. The plate was shaken for 10 min and the absorbance was measured at 570 nm on a microplate reader (ELX808IU, Bio-tek Instruments Inc, USA). Each sample was performed in triplicate, and the entire experiment was repeated three times. The cell viability of NIR-CPS (0  $\mu$ M, 5  $\mu$ M, 10  $\mu$ M, 15  $\mu$ M, 20  $\mu$ M) at 0 h, 6 h, 12 h, 18 h, 24 h and 48 h further demonstrated that the NIR-CPS was of low toxicity to cultured MCF-7 cells.

### **Preparation of the test solution.**

(1) NIR-CPS stock solution preparation: NIR-CPS (6.47 mg, 0.01 mmol) was dissolved into DMSO (10 mL) to get 1.0 mM stock solution.

(2) Na<sub>2</sub>S<sub>4</sub> stock solution preparation: Na<sub>2</sub>S<sub>4</sub> (17.42 mg, 0.1 mmol) was dissolved in 10 mL 20 mM PBS (pH= 7.4) solution under nitrogen. The resulting solution was 10 mM Na<sub>2</sub>S<sub>4</sub>, which was then diluted to 1.0 mM-100  $\mu$ M stock solution for general use. The solution was freshly prepared before each use.

(3) Na<sub>2</sub>S<sub>2</sub> stock solution preparation: Na<sub>2</sub>S<sub>2</sub> was prepared according to previous method<sup>3</sup>. Na<sub>2</sub>S<sub>2</sub> (11.01 mg, 0.1 mmol) was dissolved in 10 mL 20 mM PBS (pH= 7.4) solution under nitrogen. The resulting solution was 10 mM Na<sub>2</sub>S<sub>2</sub>, which was then diluted to 1.0 mM-100  $\mu$ M stock solution for general use. The solution was freshly prepared before each use.

(4) Na<sub>2</sub>S stock solution preparation<sup>4</sup>: 5 mg EDTA was dissolved in 10 mL DI H<sub>2</sub>O in a 25 mL Schlenk tube. The solution was purged vigorously with nitrogen for 15 min. Then 24.0 mg sodium sulfide (Na<sub>2</sub>S·9H<sub>2</sub>O) was dissolved in the solution under nitrogen. The resulting solution was 10 mM Na<sub>2</sub>S, which was then diluted to 1.0 mM-100  $\mu$ M stock solution for general use.

(5) CTAB stock solution: 3.64 mg CTAB (Hexadecyl trimethyl ammonium bromide) was dissolved in 10 mL 20 mM PBS (pH= 7.4).

(6) Cys (L-Cysteine) stock solution preparation: Cys (12.0 mg, 0.1 mmol) was dissolved into DI H<sub>2</sub>O (10 mL) to get 10.0 mM stock solution, which was then diluted to 1.0 mM and 100  $\mu$ M solution for general use.

(7) Hcy (Homocysteine) stock solution preparation: Hcy (13.5 mg, 0.1 mmol) was dissolved into DI H<sub>2</sub>O (10 mL) to get 10.0 mM stock solution, which was then diluted to 1.0 mM and 100  $\mu$ M solution for general use.

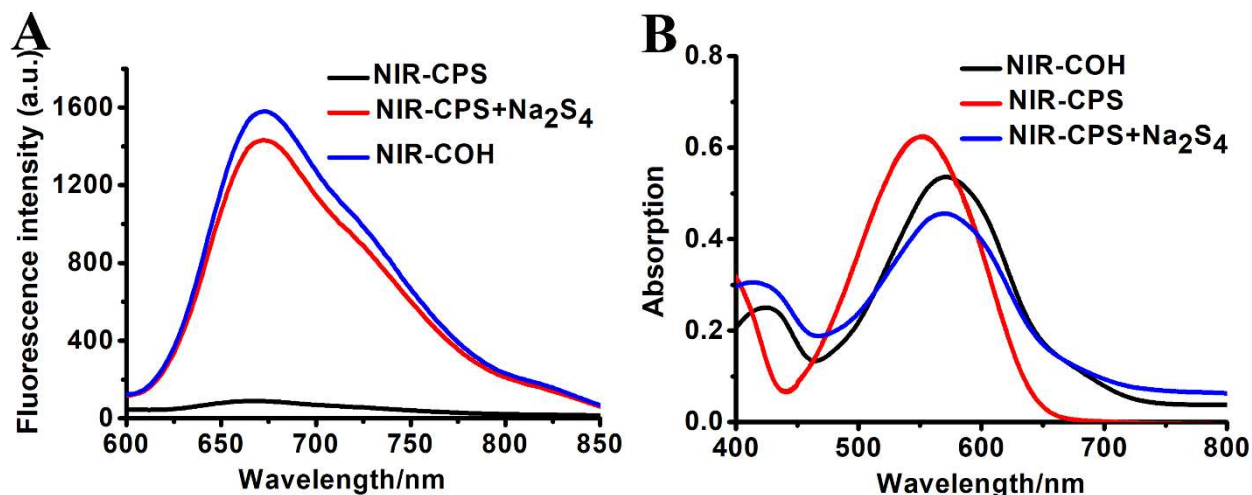
(8) GSH (Glutathione) stock solution preparation: GSH (30.7 mg, 0.1 mmol) was dissolved into DI H<sub>2</sub>O (10 mL) to get 10.0 mM stock solution, which was then diluted to 1.0 mM and 100  $\mu$ M solution for general use.

(9) Stock solutions of other reactive sulfur species, including GSSG, S<sub>8</sub>, Na<sub>2</sub>S<sub>2</sub>O<sub>3</sub>, Na<sub>2</sub>SO<sub>3</sub>, Na<sub>2</sub>SO<sub>4</sub>, Cys-polysulfide,<sup>5,6</sup> NaHSO<sub>3</sub> and S-nitroso glutathione were prepared in DI H<sub>2</sub>O. The stock solution of CH<sub>3</sub>SSSCH<sub>3</sub> was prepared in CH<sub>3</sub>CN. S<sub>8</sub> stocking solution was prepared with ethanol.

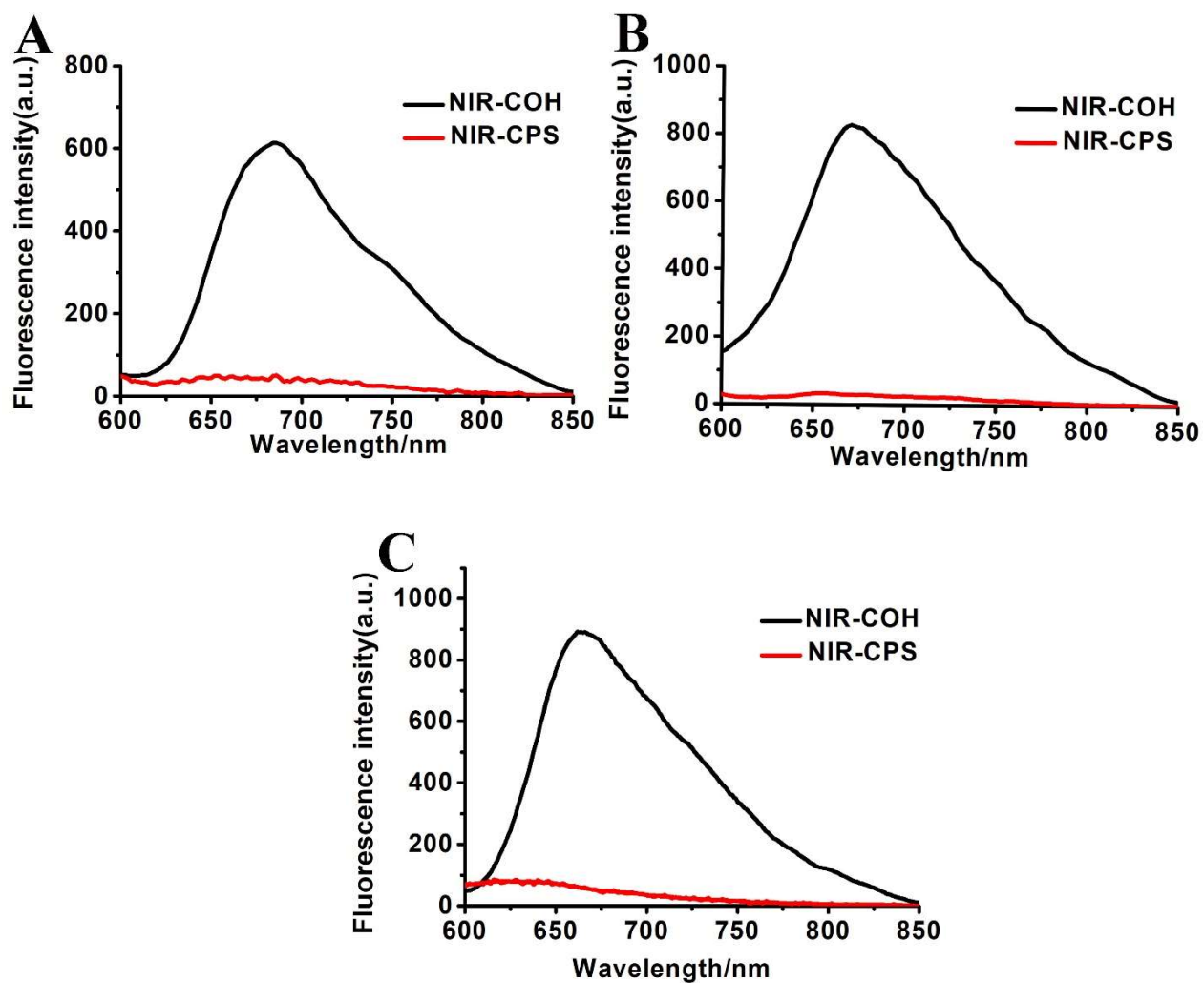
(10) Stock solutions of other biological analytes  $\text{H}_2\text{O}_2$ ,  $\text{ClO}^-$ ,  $^t\text{BuOOH}$ ,  $\cdot\text{OH}$ ,  $^1\text{O}_2$ ,  $\text{O}_2^{\cdot-}$ ,  $\text{NO}_2^-$ ,  $\text{ONOO}^-$ ,  $\text{NO}$ ,  $\text{NO}_3^-$ ,  $\text{Na}^+$ ,  $\text{K}^+$ ,  $\text{Cu}^{2+}$ ,  $\text{Ca}^{2+}$ ,  $\text{Mg}^{2+}$ ,  $\text{Zn}^{2+}$ ,  $\text{Fe}^{3+}$ ,  $\text{Fe}^{2+}$ ,  $\text{CO}_3^{2-}$ ,  $\text{HCO}_3^-$ ,  $\text{Cl}^-$ ,  $\text{Br}^-$ ,  $\text{I}^-$ ,  $\text{HPO}_4^{2-}$ ,  $\text{H}_2\text{PO}_4^-$ ,  $\text{OAc}^-$ , glucose and ascorbic acid were prepared in DI  $\text{H}_2\text{O}$ . Superoxide radicals ( $\text{O}_2^{\cdot-}$ ) were generated according to the previous reported method.<sup>7</sup>  $\cdot\text{OH}$  was generated by Fenton reaction between  $\text{Fe}^{\text{II}}(\text{EDTA})$  and  $\text{H}_2\text{O}_2$  quantitatively.<sup>8</sup>  $\text{NO}$  is generated in form of 3-(Aminopropyl)-1-hydroxy-3-isopropyl-2-oxo-1-triazene (NOC-5, 50  $\mu\text{mol/ml}$ ).  $\text{NO}_2^-$  was provided by  $\text{NaNO}_2$ .

## References

1. Qingxin Han, Zuolin Mou, Haihong Wang, Xiaoliang Tang, Zhe Dong, Li Wang, Xue Dong, Weisheng Liu. Highly selective and sensitive one- and two-photon ratiometric fluorescent probe for intracellular hydrogen polysulfide sensing. *Anal Chem.* 2016, 88(14):7206-7212.
2. Bishnu Prasad Joshi, Junwon Park, Wan In Lee, Keun-Hyeung Lee. Ratiometric and turn-on monitoring for heavy and transition metal ions in aqueous solution with a fluorescent peptide sensor. *Talanta.* 2009, 78, 903-909.
3. Toshikazu Takata, Daisaku Saeki, Yoshimasa Makita, Nobuo Yamada, Nobuhiro Kihara. Aromatic hydrocarbon-catalyzed direct reaction of sulfur and sodium in a heterogeneous system: selective and facile synthesis of sodium monosulfide and disulfide. *Inorg Chem.* 2003, 42(12):3712-3714.
4. Yong Qian, Ling Zhang, Shuting Ding, Xin Deng, Chuan He, Xi Emily Zheng, Hai-Liang Zhua and Jing Zhao. A fluorescent probe for rapid detection of hydrogen sulfide in blood plasma and brain tissues in mice. *Chem. Sci.*, 2012, 3, 2920-2923.
5. Wei Chen, Chunrong Liu, Bo Peng, Yu Zhao, Armando Pacheco, Ming Xian. New fluorescent probes for sulfane sulfurs and the application in bioimaging. *Chem Sci.* 2013, 4(7):2892-2896.
6. Kristina L Stensaas, Arnold S Brownell, Seema Ahuja, J. Kaiser Harriss, Samuel R. Herman. Competitive oxidations of dibenzyl trisulfide vs. substituted aryl polysulfides. *J. Sulfur. Chem.* 2008, 29, 433-443.
7. Ravindra L Arudi, Augustine O. Allen BenonH. J Bielski. Some observations on the chemistry of  $\text{KO}_2$ -DMSO solutions. *FEBS. Lett.* 1981, 135, 265-267.
8. B Halliwell, J M Gutteridge. Oxygen free radicals and iron in relation to biology and medicine: some problems and concepts. *Arch. Biochem. Biophys.* 1986, 246, 501-514.

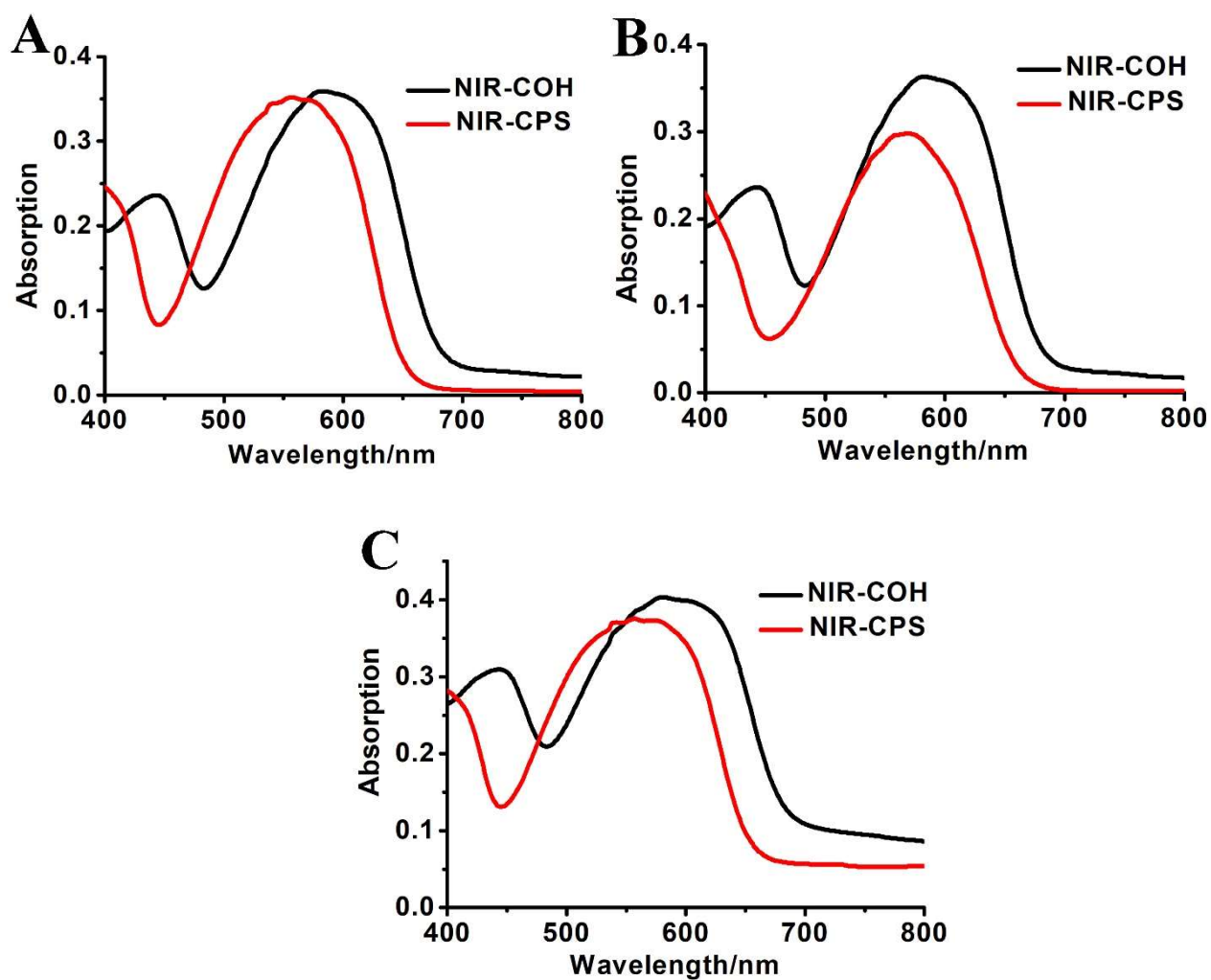


**Figure S1.** (A) Fluorescence spectra of NIR-COH, NIR-CPS and Na<sub>2</sub>S<sub>4</sub> + NIR-CPS in PBS buffer (20 mM, pH = 7.4, 1 % DMSO, containing 1 mM CTAB). (B) Absorption spectra of NIR-COH, NIR-CPS and Na<sub>2</sub>S<sub>4</sub> + NIR-CPS in PBS buffer (20 mM, pH = 7.4, 1 % DMSO, containing 1 mM CTAB).

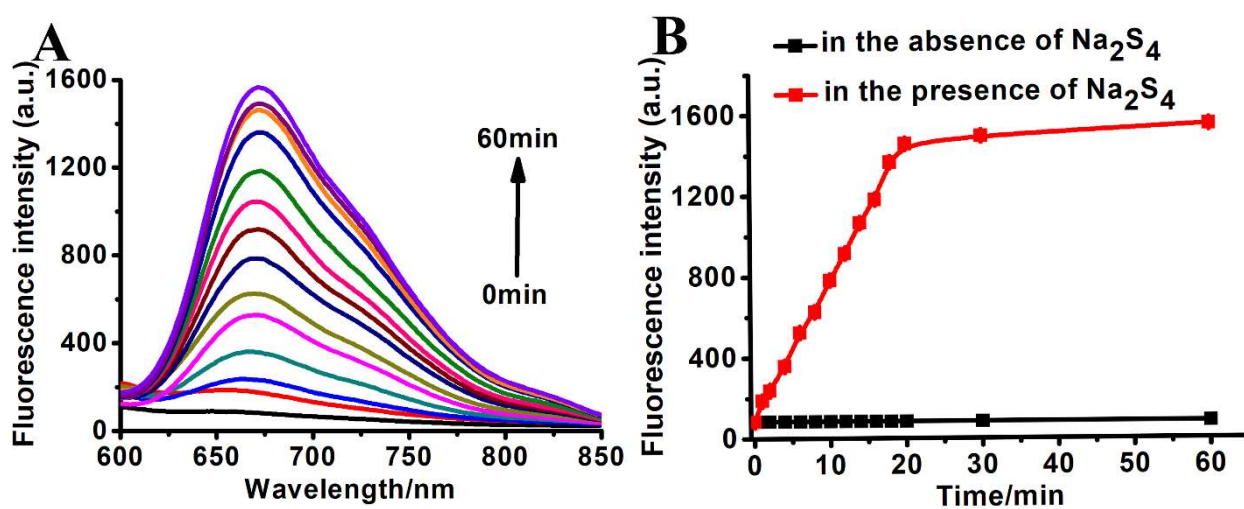


**Figure S2.** Fluorescence spectra of NIR-COH (10  $\mu$ M) and NIR-CPS (10  $\mu$ M) in PBS buffer (20 mM, pH = 7.4, 1 % DMSO) (A), DMSO (B), Acetonitrile (C).



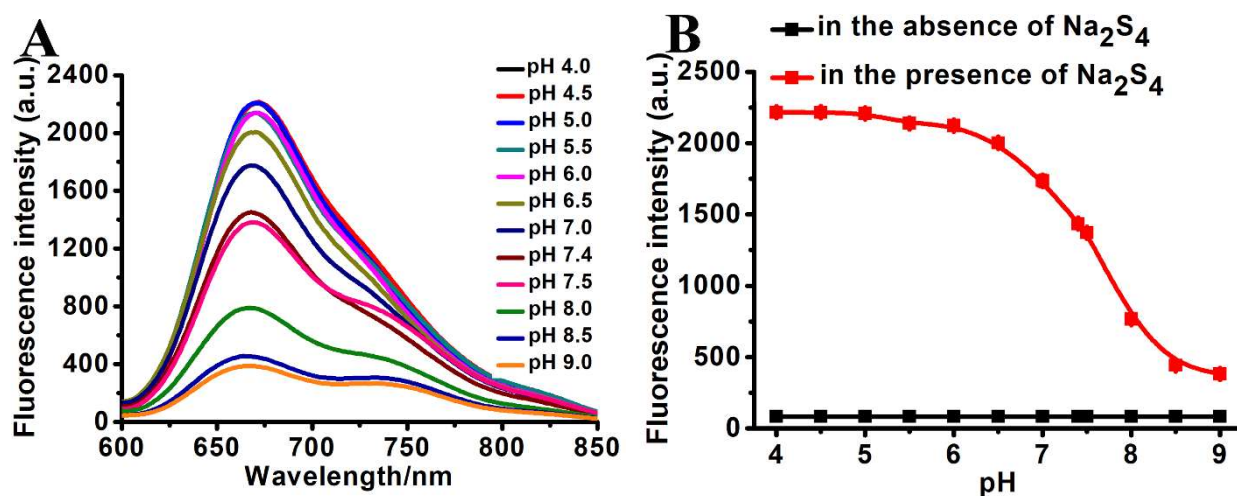


**Figure S3.** Absorption spectra of NIR-COH (10  $\mu\text{M}$ ) and NIR-CPS (10  $\mu\text{M}$ ) in PBS buffer (20 mM, pH = 7.4, 1 % DMSO) (A), DMSO (B), Acetonitrile (C).

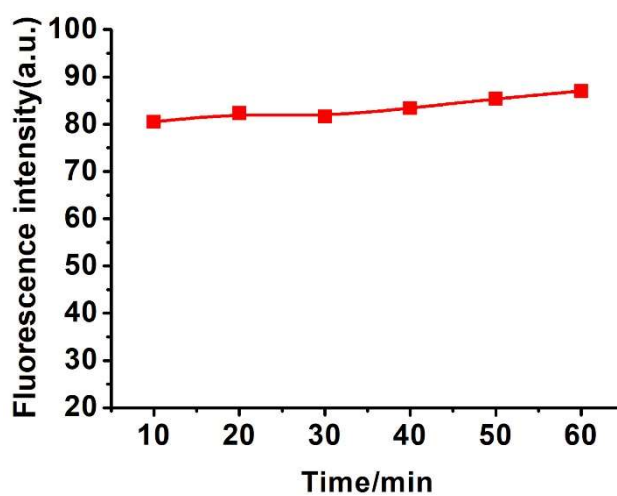


**Figure S4.** (A) Fluorescence spectra of NIR-CPS (10  $\mu\text{M}$ ) with  $\text{Na}_2\text{S}_4$  (100  $\mu\text{M}$ ) in PBS buffer (20 mM, pH = 7.4, 1 % DMSO, containing 1 mM CTAB) at 37  $^\circ\text{C}$  for 0, 1, 2, 4, 6, 8, 10, 12, 14, 16, 18, 20, 30 and 60 min. (B) Time profile of NIR-CPS (10  $\mu\text{M}$ ) toward  $\text{Na}_2\text{S}_4$  (100  $\mu\text{M}$ ) in PBS buffer (20 mM, pH = 7.4, 1% DMSO, containing 1 mM CTAB) at 37

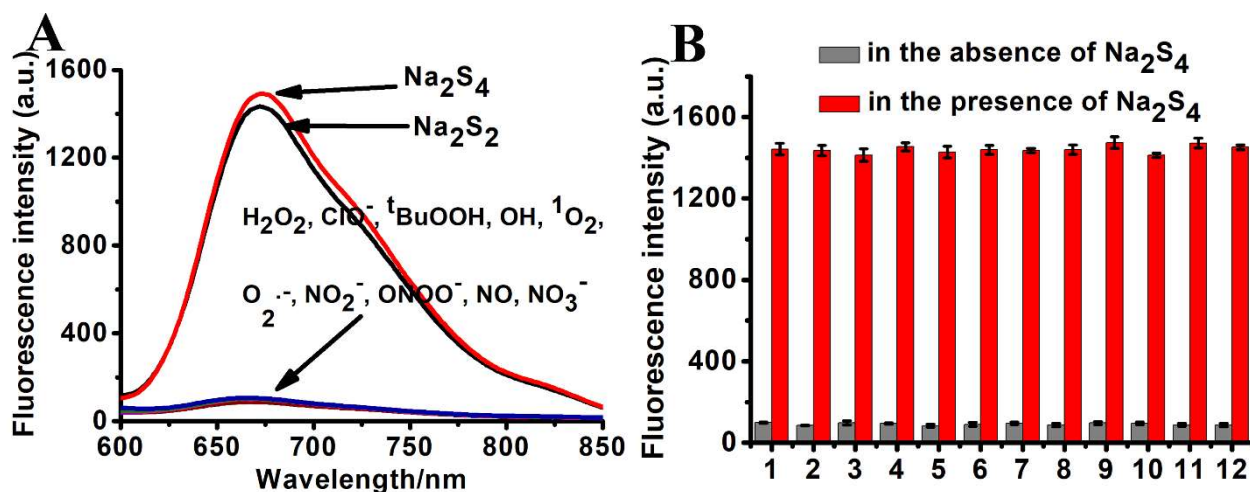
°C for 0, 1, 2, 4, 6, 8, 10, 12, 14, 16, 18, 20, 30 and 60 min. Data are presented as the mean  $\pm$  SD (n = 3).



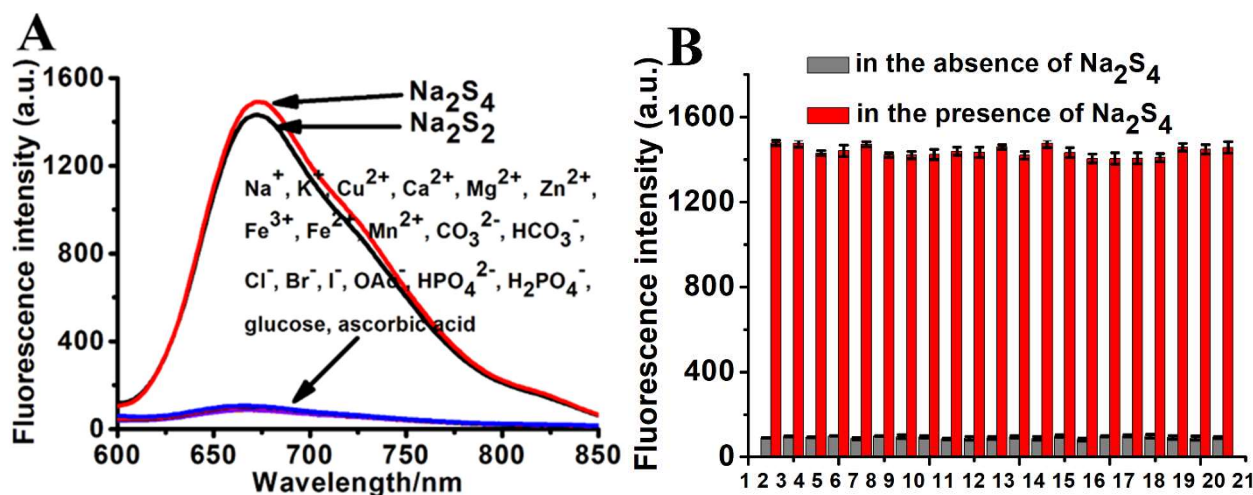
**Figure S5.** (A) Fluorescence spectra of NIR-CPS (10  $\mu$ M) with Na<sub>2</sub>S<sub>4</sub> (100  $\mu$ M) in different pH buffer (20 mM, pH 4.0, 4.5, 5.0, 5.5, 6.0, 6.5, 7.0, 7.4, 7.5, 8.0, 8.5, and 9.0, 1% DMSO, containing 1 mM CTAB) at 37 °C for 30 min. (B) Fluorescence responses of NIR-CPS (10  $\mu$ M) with Na<sub>2</sub>S<sub>4</sub> (100  $\mu$ M) in different pH buffer (20 mM, pH 4.0, 4.5, 5.0, 5.5, 6.0, 6.5, 7.0, 7.4, 7.5, 8.0, 8.5, and 9.0, 1% DMSO, containing 1 mM CTAB) at 37 °C for 30 min.



**Figure S6.** Fluorescence intensities of NIR-CPS (10  $\mu$ M) alone in PBS buffer (20 mM, pH = 7.4, 1 % DMSO) for 10, 20, 30, 40, 50 and 60 min.

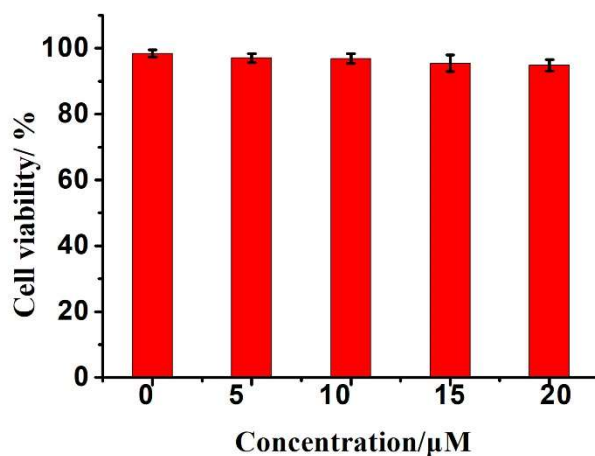


**Figure S7.** The selectivity of NIR-CPS for  $\text{H}_2\text{S}_n$ . (A) Fluorescence spectra of NIR-CPS (10  $\mu\text{M}$ ) towards  $\text{Na}_2\text{S}_4$  (100  $\mu\text{M}$ ),  $\text{Na}_2\text{S}_2$  (100  $\mu\text{M}$ ) and various reactive oxygen species ( $\text{H}_2\text{O}_2$ ,  $\text{ClO}^-$ ,  $^t\text{BuOOH}$ ,  $\cdot\text{OH}$ ,  $^1\text{O}_2$ ,  $\text{O}_2^{\cdot-}$ ,  $\text{NO}_2^-$ ,  $\text{ONOO}^-$ ,  $\text{NO}$ ,  $\text{NO}_3^-$ ) in PBS buffer (20 mM, pH = 7.4, 1 % DMSO, containing 1 mM CTAB) at 37  $^\circ\text{C}$  for 30 min. (B) Fluorescence responses of NIR-CPS (10  $\mu\text{M}$ ) towards  $\text{Na}_2\text{S}_4$  (100  $\mu\text{M}$ ),  $\text{Na}_2\text{S}_2$  (100  $\mu\text{M}$ ) and various reactive sulfur species at 37  $^\circ\text{C}$  for 30 min. In each group, the red bars represent relative responses at 670 nm of NIR-CPS to ROS, RNS and the mixture of ROS/RNS with 100  $\mu\text{M}$   $\text{Na}_2\text{S}_4$ , respectively. 1. blank +  $\text{Na}_2\text{S}_4$  (100  $\mu\text{M}$ ); 2. blank +  $\text{Na}_2\text{S}_2$  (100  $\mu\text{M}$ ); 3.  $\text{H}_2\text{O}_2$  (100  $\mu\text{M}$ ) +  $\text{Na}_2\text{S}_4$  (100  $\mu\text{M}$ ); 4.  $\text{OCl}^-$  (100  $\mu\text{M}$ ) +  $\text{Na}_2\text{S}_4$  (100  $\mu\text{M}$ ); 5.  $^t\text{BuOOH}$  (100  $\mu\text{M}$ ) +  $\text{Na}_2\text{S}_4$  (100  $\mu\text{M}$ ); 6.  $\cdot\text{OH}$  (100  $\mu\text{M}$ ) +  $\text{Na}_2\text{S}_4$  (100  $\mu\text{M}$ ); 7.  $^1\text{O}_2$  (100  $\mu\text{M}$ ) +  $\text{Na}_2\text{S}_4$  (100  $\mu\text{M}$ ); 8.  $\text{O}_2^{\cdot-}$  (100  $\mu\text{M}$ ) +  $\text{Na}_2\text{S}_4$  (100  $\mu\text{M}$ ); 9.  $\text{NO}_2^-$  (100  $\mu\text{M}$ ) +  $\text{Na}_2\text{S}_4$  (100  $\mu\text{M}$ ); 10.  $\text{ONOO}^-$  (100  $\mu\text{M}$ ) +  $\text{Na}_2\text{S}_4$  (100  $\mu\text{M}$ ); 11.  $\text{NO}$  (100  $\mu\text{M}$ ) +  $\text{Na}_2\text{S}_4$  (100  $\mu\text{M}$ ); 12.  $\text{NO}_3^-$  (100  $\mu\text{M}$ ) +  $\text{Na}_2\text{S}_4$  (100  $\mu\text{M}$ ). Data are presented as the mean  $\pm$  SD ( $n = 3$ ).

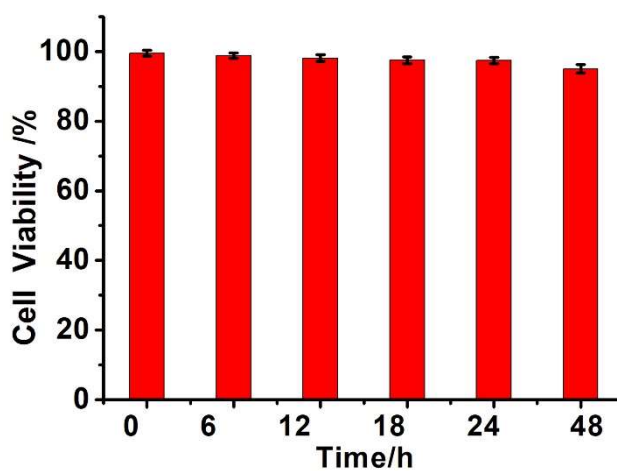


**Figure S8.** The selectivity of NIR-CPS for  $\text{H}_2\text{S}_n$ . (A) Fluorescence spectra of NIR-CPS (10  $\mu\text{M}$ ) towards  $\text{Na}_2\text{S}_4$  (100  $\mu\text{M}$ ),  $\text{Na}_2\text{S}_2$  (100  $\mu\text{M}$ ) and various ions ( $\text{Na}^+$ ,  $\text{K}^+$ ,  $\text{Cu}^{2+}$ ,  $\text{Ca}^{2+}$ ,  $\text{Mg}^{2+}$ ,  $\text{Zn}^{2+}$ ,  $\text{Fe}^{3+}$ ,  $\text{Fe}^{2+}$ ,  $\text{Mn}^{2+}$ ,  $\text{CO}_3^{2-}$ ,  $\text{HCO}_3^-$ ,  $\text{Cl}^-$ ,  $\text{Br}^-$ ,  $\text{I}^-$ ,  $\text{OAc}^-$ ,  $\text{HPO}_4^{2-}$ ,  $\text{H}_2\text{PO}_4^-$ , glucose, ascorbic acid, 1 mM) in PBS buffer (20 mM, pH = 7.4, 1% DMSO, containing 1 mM CTAB) at 37  $^\circ\text{C}$  for 30 min. (B) Fluorescence responses of NIR-CPS (10  $\mu\text{M}$ ) towards  $\text{Na}_2\text{S}_4$  (100  $\mu\text{M}$ ),  $\text{Na}_2\text{S}_2$  (100  $\mu\text{M}$ ) and various ions at 37  $^\circ\text{C}$  for 30 min. In each group, the red bars represent relative responses at 670 nm of NIR-CPS to ions and the mixture of ions with 100  $\mu\text{M}$   $\text{Na}_2\text{S}_4$ , respectively. 1. blank +  $\text{Na}_2\text{S}_4$  (100  $\mu\text{M}$ ); 2. blank +  $\text{Na}_2\text{S}_4$  (100  $\mu\text{M}$ ); 3.  $\text{Na}^+$  (1 mM) +  $\text{Na}_2\text{S}_4$  (100  $\mu\text{M}$ ); 4.  $\text{K}^+$  (1 mM) +  $\text{Na}_2\text{S}_4$  (100  $\mu\text{M}$ ); 5.  $\text{Cu}^{2+}$  (1 mM) +  $\text{Na}_2\text{S}_4$  (100  $\mu\text{M}$ ); 6.  $\text{Ca}^{2+}$  (1 mM) +

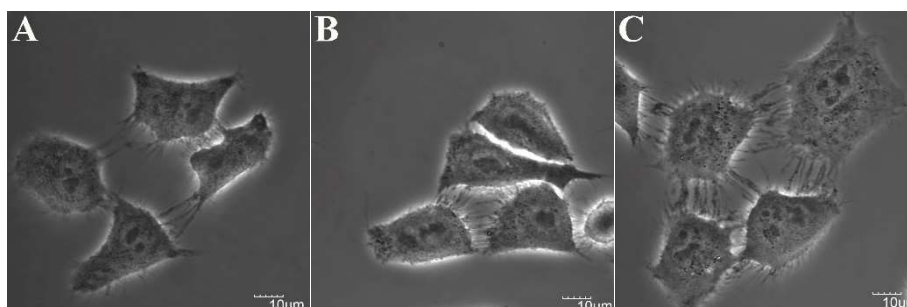
Na<sub>2</sub>S<sub>4</sub> (100 μM); 7. Mg<sup>2+</sup> (1 mM)+ Na<sub>2</sub>S<sub>4</sub> (100 μM); 8. Zn<sup>2+</sup> (1 mM)+ Na<sub>2</sub>S<sub>4</sub> (100 μM); 9. Fe<sup>3+</sup> (1 mM)+ Na<sub>2</sub>S<sub>4</sub> (100 μM); 10. Fe<sup>2+</sup> (1 mM)+ Na<sub>2</sub>S<sub>4</sub> (100 μM); 11. Mn<sup>2+</sup> (1 mM)+ Na<sub>2</sub>S<sub>4</sub> (100 μM); 12. CO<sub>3</sub><sup>2-</sup> (1 mM)+ Na<sub>2</sub>S<sub>4</sub> (100 μM); 13. HCO<sub>3</sub><sup>-</sup> (1 mM)+ Na<sub>2</sub>S<sub>4</sub> (100 μM); 14. Cl<sup>-</sup> (1 mM)+ Na<sub>2</sub>S<sub>4</sub> (100 μM); 15. Br<sup>-</sup> (1 mM)+ Na<sub>2</sub>S<sub>4</sub> (100 μM); 16. I<sup>-</sup> (1 mM)+ Na<sub>2</sub>S<sub>4</sub> (100 μM); 17. HPO<sub>4</sub><sup>2-</sup> (1 mM)+ Na<sub>2</sub>S<sub>4</sub> (100 μM); 18. H<sub>2</sub>PO<sub>4</sub><sup>-</sup> (1 mM)+ Na<sub>2</sub>S<sub>4</sub> (100 μM); 19. OAc<sup>-</sup> (1 mM)+ Na<sub>2</sub>S<sub>4</sub> (100 μM); 20. glucose (1 mM)+ Na<sub>2</sub>S<sub>4</sub> (100 μM); 21. ascorbic acid(1 mM)+ Na<sub>2</sub>S<sub>4</sub> (100 μM). Data are presented as the mean ± SD (*n* = 3).



**Figure S9.** Cell viability of different concentrations of NIR-CPS (0 μM, 5 μM, 10 μM, 15 μM, 20 μM) at 24 h in MCF-7 cells. Data are presented as the mean ± SD (*n* = 3).



**Figure S10.** Cell viability of NIR-CPS (10 μM) at different times (0 h, 6 h, 12 h, 18 h, 24 h, 48 h) in MCF-7 cells. Data are presented as the mean ± SD (*n* = 3).



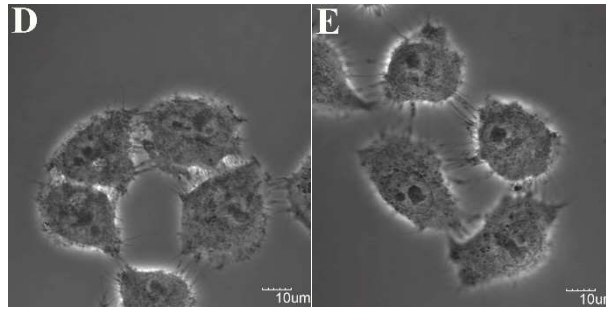


**Figure S11.** The corresponding bright images of Fig. 3, panels A, B, C, D and E.

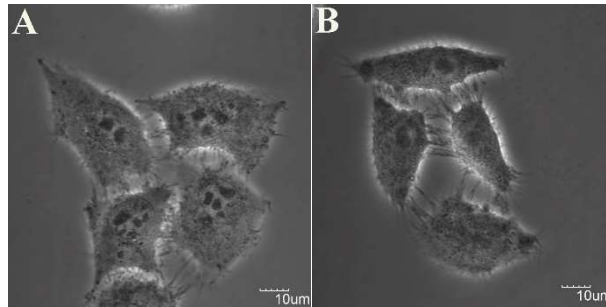


**Figure S12.** The corresponding bright images of Fig. 4, panels A and B.

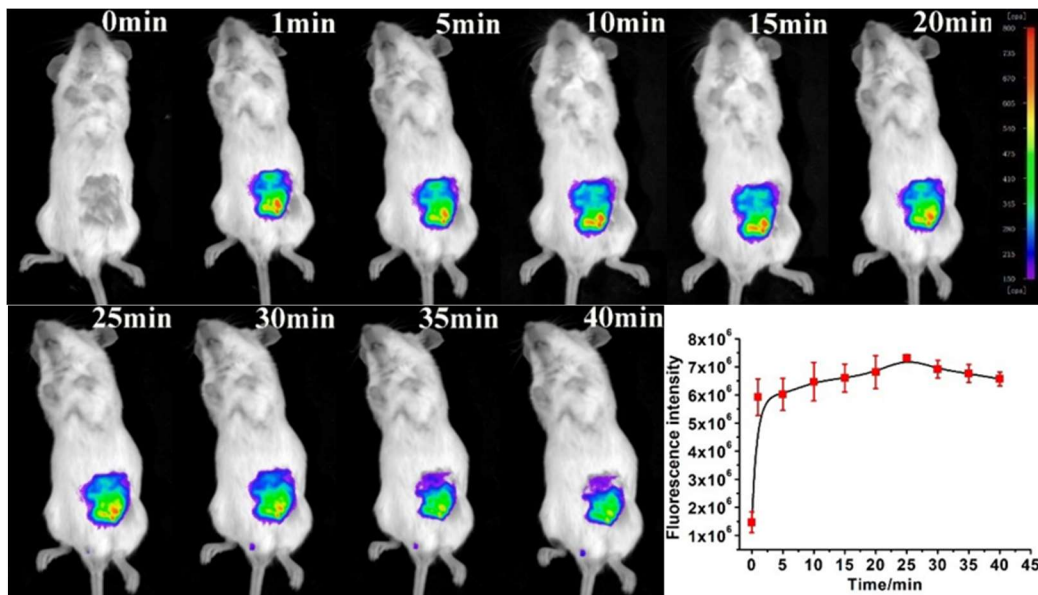


**Figure S13.** Representative fluorescence images of visualizing  $H_2S_n$  levels at different times in living mice using NIR-CPS. The mice were i.p. injected with LPS (10  $\mu\text{g}/\text{mL}$ , 100  $\mu\text{L}$  in saline) for 24h, followed by i.p. injection of NIR-CPS (2 mM, 100  $\mu\text{L}$  DMSO). Images were taken after incubation of NIR-CPS at: 0 min; 1 min; 5 min; 10 min; 15 min; 20 min; 25 min; 30 min; 35 min; 40 min. Quantification of the fluorescence emission intensities from the abdominal area of the mice of the above groups. Data are presented as the mean  $\pm$  SD ( $n = 3$ ).

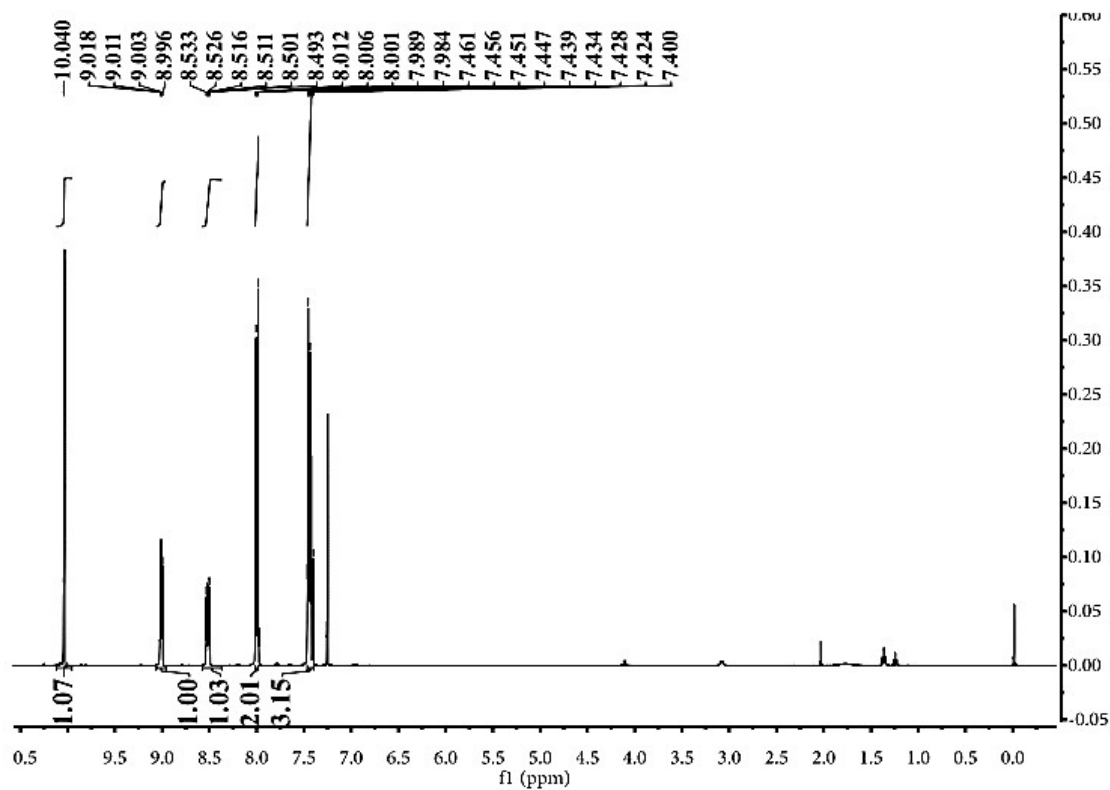


Figure S14. <sup>1</sup>H NMR spectrum of compound 2.

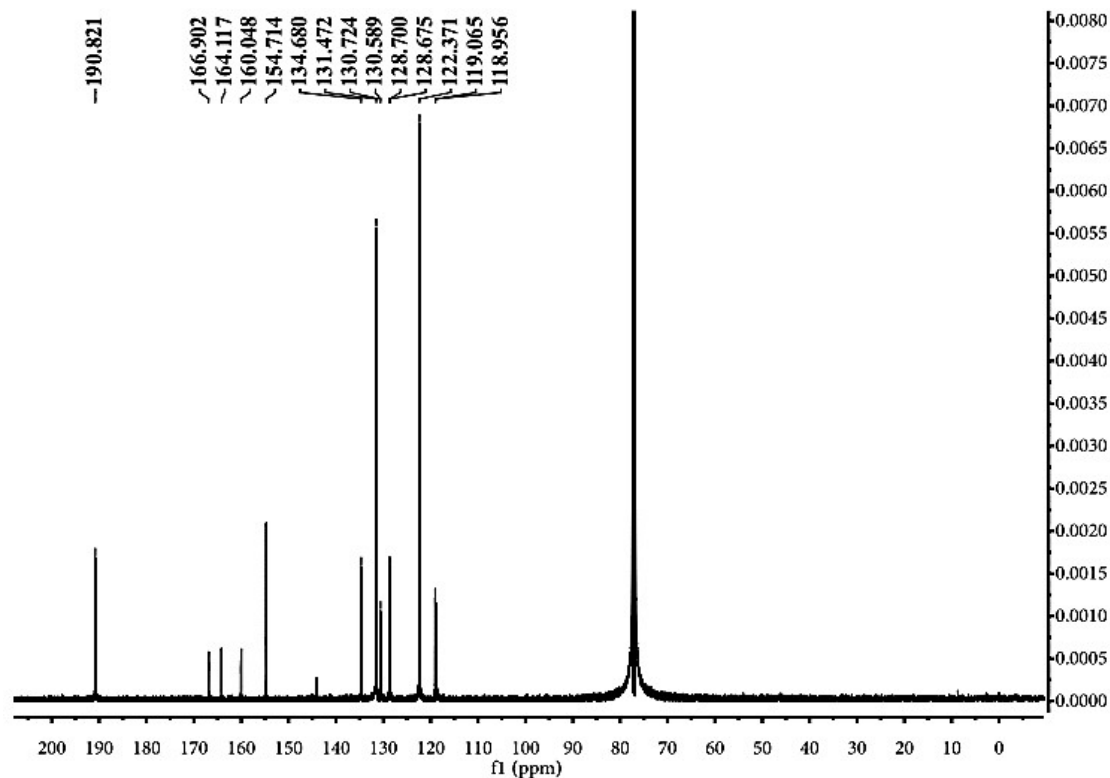


Figure S15. <sup>13</sup>C NMR spectrum of compound 2.



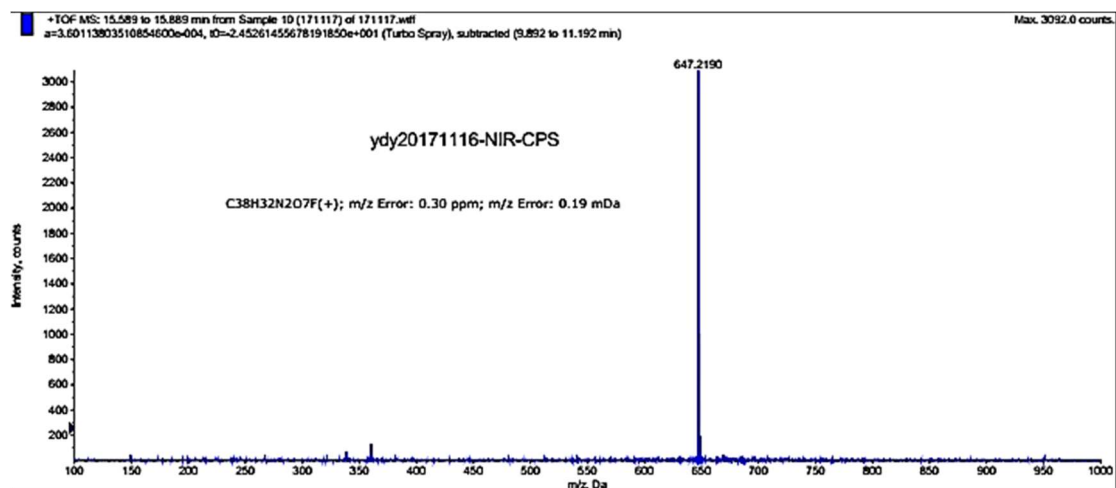


Figure S18. HRMS identification of NIR-CPS (calculated for C<sub>38</sub>H<sub>32</sub>N<sub>2</sub>O<sub>7</sub> (M)<sup>+</sup> 647.2118; found 647.2190).

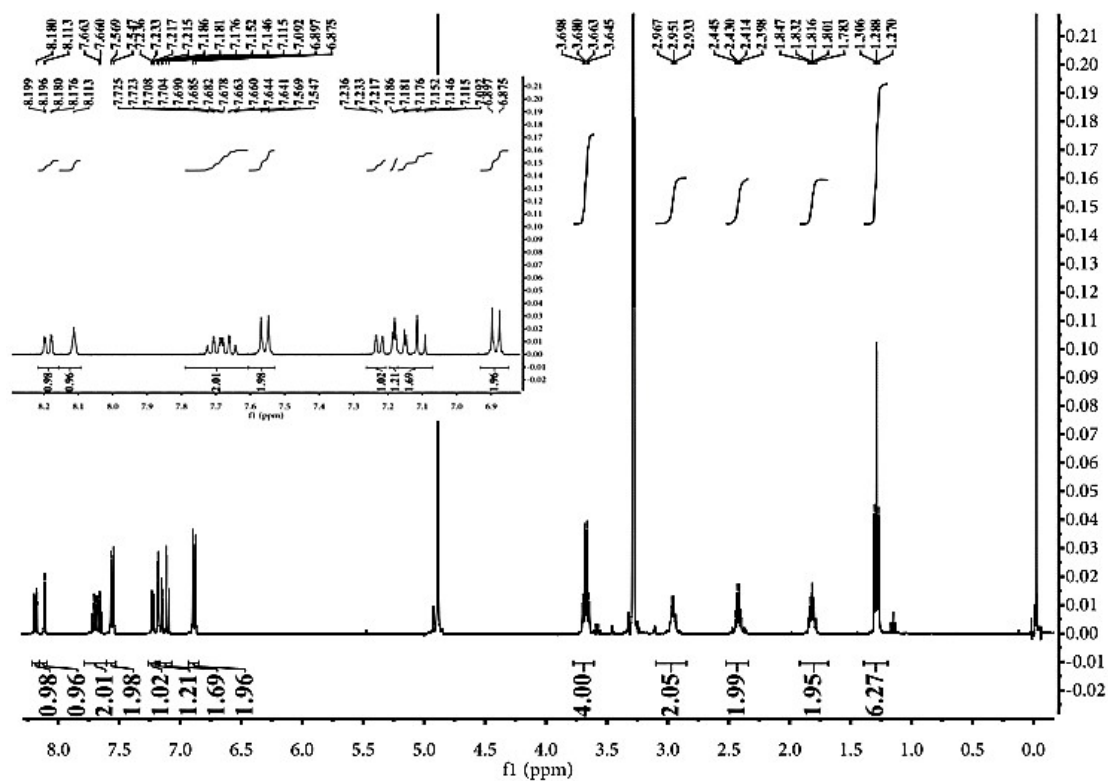


Figure S19. <sup>1</sup>H NMR spectrum of compound NIR-COH.



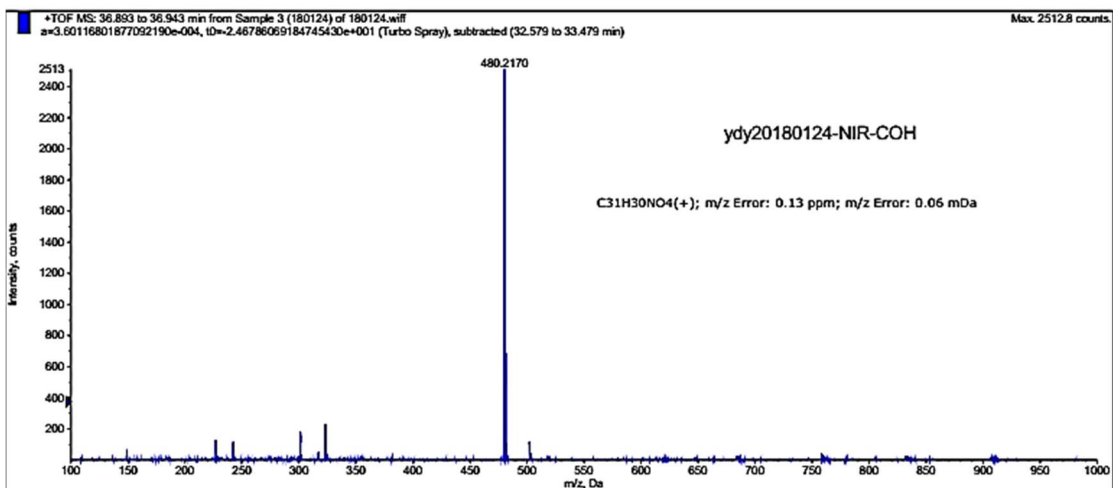


Figure S20. HRMS identification of NIR-COH (calculated for  $C_{31}H_{30}NO_4$  ( $M$ ) $^+$ 480.2169; found 480.2170).

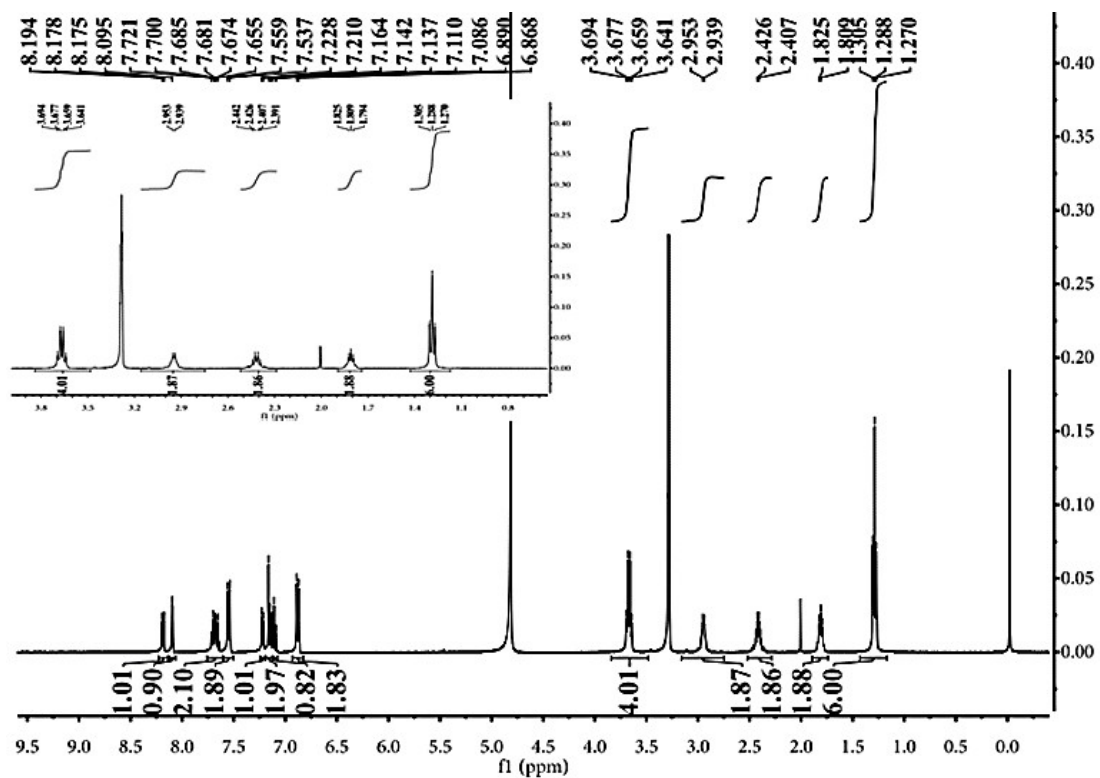
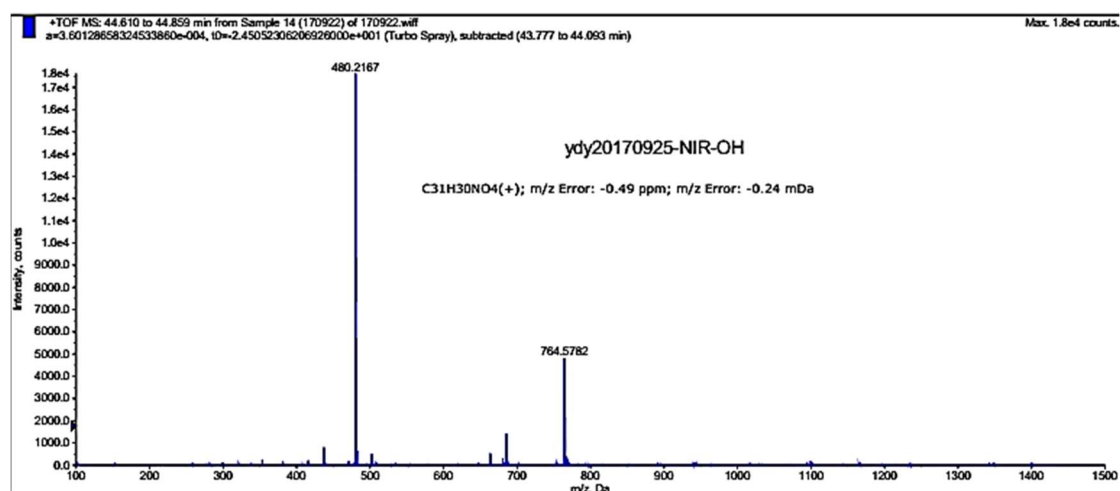
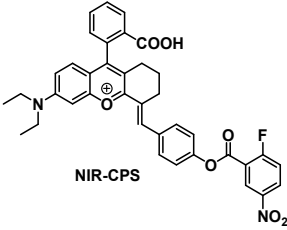


Figure S18.  $^1H$  NMR spectra of the isolated fluorescent product of NIR-CPS +  $Na_2S_4$ .

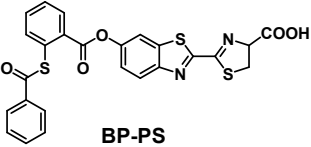
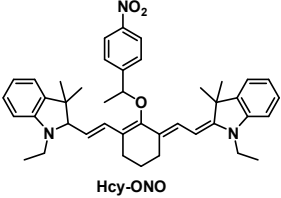
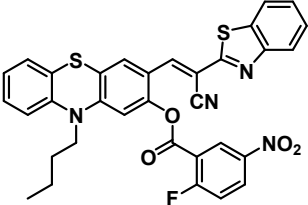
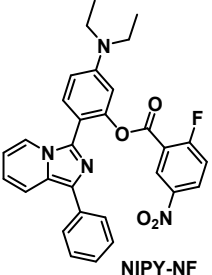
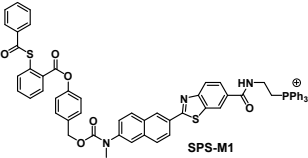
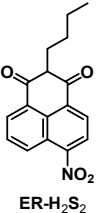
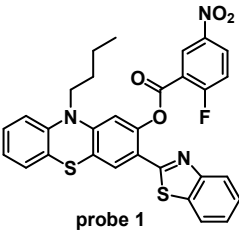
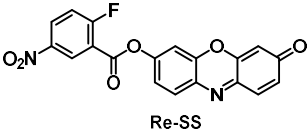


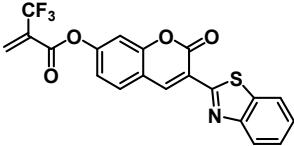
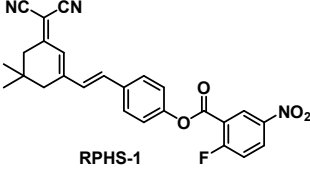
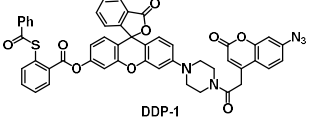
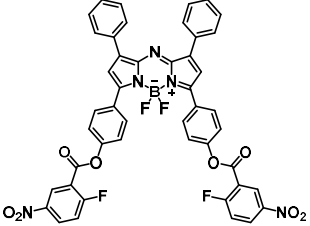
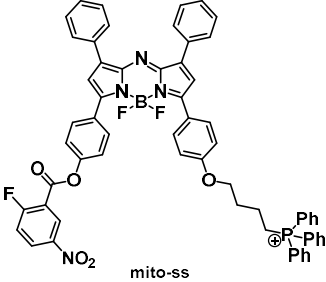
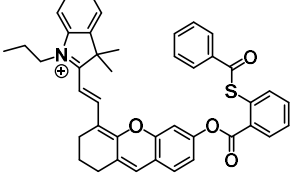
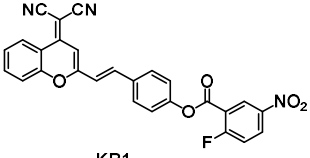
**Figure S22.** HR-MS identification of isolated fluorescent product of NIR-CPS + Na<sub>2</sub>S<sub>4</sub> (calculated for C<sub>31</sub>H<sub>30</sub>NO<sub>4</sub> (M)<sup>+</sup>480.2169; found 480.2167).

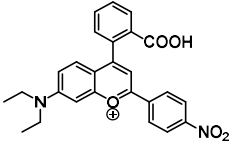
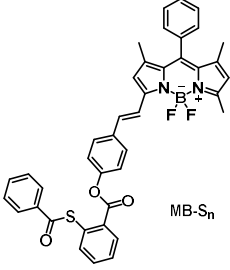
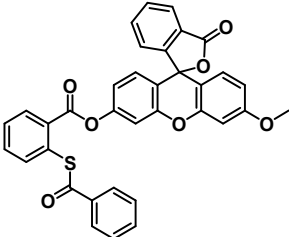
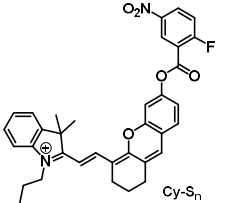
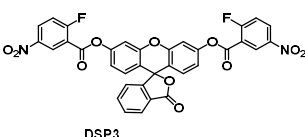
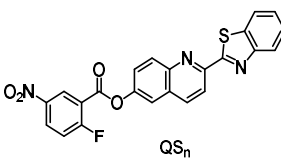
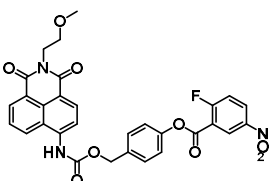
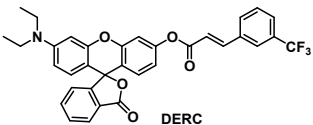
**Table S1. Summary of the reported H<sub>2</sub>S<sub>n</sub> fluorescent probes**

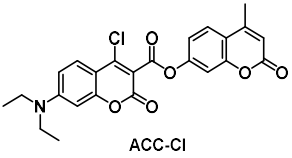
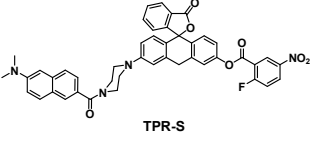
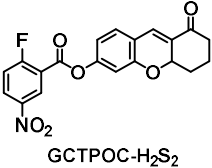
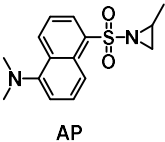
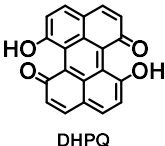
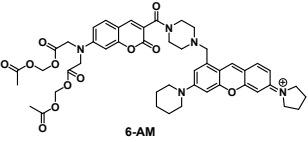
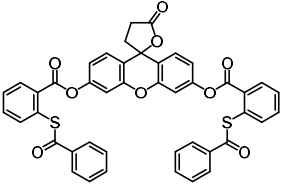
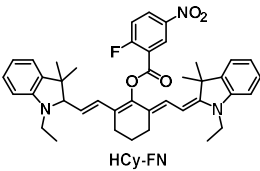
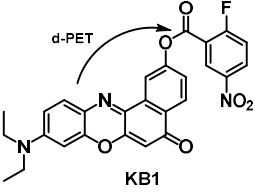
Probes	Reference	$\lambda_{\text{abs}}/\lambda_{\text{em}}$ (nm)	Stokes shift (nm)	Detection limit (nM)	Applicati on
 NIR-CPS	This paper	570/670	100	18	tumor-bearing mice
	Spectrochim Acta A Mol Biomol Spectrosc, 2020, 227: 117579.	338/502	137	500	Cells
	Biomater Sci, 2020, 8(1): 224-231.	300/478	178	1	Tissues
	Spectrochim Acta A Mol Biomol Spectrosc, 2019, 223: 117295.	比率计 F <sub>574</sub> /F <sub>618</sub>	-	57	Cells

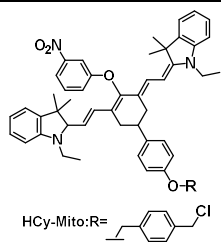


 <p><b>BP-PS</b></p>	Chem. Commun, 2019, 55(31): 4487-4490.	-	Bioluminescent Probe	30	Mice
 <p><b>Hcy-ONO</b></p>	Anal Chem, 2019, 91(12): 7774-7781.	$\lambda_{em} = 635$	no	100	Mice
 <p><b>PZC-Sn</b></p>	Sens Actuators B Chem, 2019, 284: 30-35.	490/620	130	1	Zebrafish
 <p><b>NIPY-NF</b></p>	Anal Chim Acta, 2019, 1056: 117-124.	305/520	215	84	Cells
 <p><b>SPS-M1</b></p>	Sens Actuators B Chem, 2019, 283: 810-819.	430/506	76	100	Mice (PD model)
 <p><b>ER-H<sub>2</sub>S<sub>2</sub></b></p>	Sens Actuators B Chem, 2019, 278: 64-72.	369/540	171	26	Zebrafish
 <p><b>probe 1</b></p>	Spectrochim Acta A Mol Biomol Spectrosc, 2019, 213: 342-346.	397/534	137	26	Zebrafish
 <p><b>Re-SS</b></p>	Analyst, 2019, 144(10): 3221-3225.	576/589	13	24	Cells

 <p><b>FP-CF3</b></p>	Anal Chem, 2018, 90(1): 881-887.	no	no	50	Cells
 <p><b>RPHS-1</b></p>	J Mater Chem B, 2018, 6(43): 7015-7020.	431/577, 655	no	43	Cells
 <p><b>DDP-1</b></p>	Angew Chem Int Ed Engl, 2016, 55(34): 9993-9996.	$\lambda_{em} = 542$	no	24	Cells
 <p><b>BD-ss</b></p>	Analyst, 2015, 140(11): 3766-3772.	707/737	30 nm	50	Mice (endogenous H <sub>2</sub> S <sub>n</sub> )
 <p><b>mito-ss</b></p>	Anal Chem, 2015, 87(7): 3631-3638.	675/730	55 nm	25	Mice (exogenous H <sub>2</sub> S <sub>n</sub> )
 <p><b>probe1</b></p>	Chem Commun, 2017, 53(62): 8759-8762.	680/708	28 nm	35	Mice
 <p><b>KB1</b></p>	Sens Actuators B Chem, 2018, 254: 222-226.	535/682	147 nm	8.2	Cells

 <p>Probe 1</p>	RSC Adv, 2016, 6(91): 88519-88526.	568/620	52 nm	75	Cells
 <p>MB-S<sub>n</sub></p>	Chem Commun, 2018, 54(30): 3735-3738.	570/584	14 nm	26	Cells
	Chem Sci, 2018, 9(25): 5556-5563.	no	no	2	Zebrafish
 <p>Cy-S<sub>n</sub></p>	J Mater Chem B, 2017, 5(14): 2574-2579.	700/720	20 nm	22	Mice
 <p>DSP3</p>	J Am Chem Soc, 2014, 136(20): 7257-7260.	$\lambda_{em} = 515$	no	71	Cells
 <p>QS<sub>n</sub></p>	Anal Chem, 2015, 87(5): 3004-3010.	362/534	172 nm	500	Zebrafish
 <p>NRT-HP</p>	Anal Chem, 2016, 88(14): 7206-7212.	432/542	110 nm	100	Tissues
 <p>DERC</p>	Sens Actuators B Chem, 2016, 232: 531-537.	$\lambda_{em} = 548$	no	400	Cells

 ACC-Cl	Sens Actuators B Chem, 2018, 258: 125-132.	421/461	40 nm	65	Cells
 TPR-S	Anal Chem, 2016, 88(23): 11892-11899.	no	no	700	Organs
 GCTPOC-H <sub>2</sub> S <sub>2</sub>	Sens Actuators B Chem, 2016, 230: 773-778.	$\lambda_{em} = 512$	no	152	Mice
 AP	Org Lett, 2015, 17(11): 2776-2779.	350/530	180 nm	300	no
 DHPQ	Talanta, 2017, 164: 529- 533.	425/490	65 nm	18.2	Cells
 6-AM	Chem Sci, 2017, 8(2): 1134-1140.	$\lambda_{em} = 584$	no	1000	Cells
 PSP-3	Angew Chem Int Ed Engl, 2015, 54(47): 13961-13965.	$\lambda_{em} = 515$	no	3	Cells
 Hcy-FN	Biomaterials, 2015, 63: 93-101.	775/794	19 nm	19	Mice
 KB1	Anal. Methods, 2017, 9: 6443-6447.	$\lambda_{em} = 655$	no	3.9	Cells



Anal Chem, 2016, 88(7):  
4122-4129.

770/780

10 nm

50

Mice